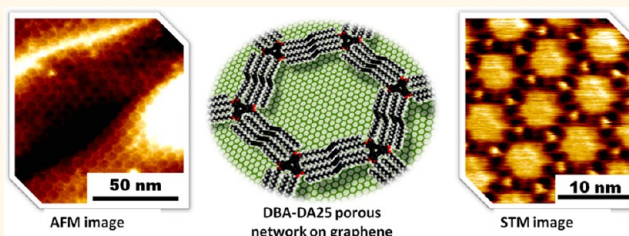# Self-Assembled Air-Stable Supramolecular Porous Networks on Graphene

Bing Li,[†,||] Kazukuni Tahara,[‡] Jinne Adisoejoso,[†] Willem Vanderlinden,[†] Kunal S. Mali,[†] Stefan De Gendt,[§,⊥] Yoshito Tobe,[‡,*] and Steven De Feyter[†,*]

[†]Department of Chemistry, Division of Molecular Imaging and Photonics, KU Leuven-University of Leuven, Celestijnenlaan 200F, B-3001 Leuven, Belgium, [‡]Division of Frontier Materials Science, Graduate School of Engineering Science, Osaka University, Toyonaka, Osaka 560-8531, Japan, [§]Department of Chemistry, Division of Molecular Design and Synthesis, KU Leuven-University of Leuven, Celestijnenlaan 200F, B-3001 Leuven, Belgium, and [⊥]IMEC, Kapeldreef 75, B-3001 Leuven, Belgium. [||]Present address: Institute of Material Research and Engineering (A*STAR), 3 Research Link, 117602, Singapore.

ABSTRACT Functionalization and modification of graphene at the nanometer scale is desirable for many applications. Supramolecular assembly offers an attractive approach in this regard, as many organic molecules form well-defined patterns on surfaces such as graphite *via* physisorption. Here we show that ordered porous supramolecular networks with different pore sizes can be readily fabricated on different graphene substrates *via* self-assembly of dehydrobenzo[12]annulene

AFM image   DBA-DA25 porous network on graphene   STM image

(DBA) derivatives at the interface between graphene and an organic liquid. Molecular resolution scanning tunneling microscopy (STM) and atomic force microscopy (AFM) investigations reveal that the extended honeycomb networks are highly flexible and that they follow the topological features of the graphene surface without any discontinuity, irrespective of the step-edges present in the substrate underneath. We also demonstrate the stability of these networks under liquid as well as ambient air conditions. The robust yet flexible DBA network adsorbed on graphene surface is a unique platform for further functionalization and modification of graphene. Identical network formation irrespective of the substrate supporting the graphene layer and the level of surface roughness illustrates the versatility of these building blocks.

KEYWORDS: self-assembly · scanning tunneling microscopy · atomic force microscopy · graphene · porous networks · supramolecular

W ithin a decade, graphene has emerged as one of the most promising nanomaterials in contemporary nanotechnology. The unique structure and remarkable properties[1−6] of graphene have boosted its use in various domains of science and technology such as nanoelectronics, catalysis, sensing, and energy storage.[7−12] Functionalization or modification of graphene is often a prerequisite to take full advantage of its unique properties.[13−17] Approaches including covalent chemical modifications[18,19] and physical treatments[20,21] have shown that it is possible to functionalize graphene and to affect its electronic properties, for instance by inducing a band gap. Nevertheless, these reaction methods often generate defects in graphene at the expense of reducing the carrier mobilities. Noncovalent functionalization *via* physisorbed self-assembled monolayers has emerged as a promising strategy,

as it preserves the pristine structure of graphene, thus conserving its excellent electrical properties.[9,10] The extended honeycomb lattice of the sp[2] carbon network of graphene enables the adsorption of a variety of molecules *via* physisorption and their assembly into ordered networks guided by weak van der Waals (vdW) interactions between graphene and the adsorbed molecules.

Several organic molecules such as 10,12-pentacosadiynoic acid (PCDA),[22] 3,4,9,10-perylenetetracarboxylic dianhydride (PTCDA),[23−27] perylenetetracarboxylic diimides (PTCDI),[25,28] copper phthalocyanine (CuPc),[29] chloroaluminum phthalocyanine (ClAlPc),[30] and cobalt phthalocyanine (CoPc)[31] form well-ordered self-assembled two-dimensional (2D) nanopatterns on graphene as visualized by scanning tunneling microscopy (STM). The deposition as well as the STM imaging of the aforementioned molecular

networks was carried out under ultra-high vacuum (UHV) conditions, which limits the scope of molecules that can be explored and integrated with graphene because of sublimation problems. Another obvious concern is the stability of molecular monolayers on graphene when exposed to ambient conditions or when graphene substrates are immersed in liquids. Such stability is absolutely essential when considering the utility of graphene-based devices in sensing applications. Furthermore, for all the systems listed above, the supramolecular networks formed on graphene consist of densely packed arrangement of molecules without leaving any void space. Porous supramolecular networks that expose nanosized areas of graphene surface could be extremely interesting since such uncovered areas could be used for further functionalization and also for trapping of guest molecules on the basis of shape and size selectivity, as previously demonstrated for nanoporous systems adsorbed on graphite.[32] Lastly, most of the studies on molecular self-assembly on graphene have dealt with a single combination of a molecule and the type of graphene surface. Given the fact that graphene can be grown on a variety of different substrates, there is a pressing need for understanding molecular self-assembly behavior on different types of graphene substrates for a single building block.

In this contribution we attempt to address the missing links outlined above as follows. We explore the use of liquid–solid interface as an alternative to UHV deposition for functionalization of the graphene surface by physisorption, using molecular systems that are incompatible with deposition under UHV conditions. In contrast to UHV deposition, the liquid–solid interface provides a relatively cheap and practically straightforward protocol for deposition of a variety of different molecules. In particular, we illustrate the formation of functional, crystalline, low-density molecular networks on graphene. These networks extend over large areas on graphene surface, and the nanosized voids in them expose the pristine graphene surface, which is available for further functionalization as well as for sensing purposes as described above. To the best of our knowledge, this is the first example of a highly ordered and extended 2D porous supramolecular network with pore size greater than 5 nm physisorbed on graphene. These nanoporous networks maintain their structural integrity and porosity even upon removal of the organic solvent from which they were formed. They remain stable for days under ambient dry conditions as well as after washing with water. Last but not the least, we illustrate the self-assembly of the same building block on three different types of graphene substrates, namely, epitaxial few-layer graphene grown on SiC (E-G/SiC),[23,25] chemical vapor deposition (CVD)-grown single-layer graphene on polycrystalline Cu film on silicon wafer (CVD-G/Cu),[33,34] and mechanically exfoliated small single-layer graphene

sheets on a mica substrate (M-G/Mica),[5] further corroborating the versatility of these building blocks under ambient conditions.

The present investigation rides on the success of numerous earlier investigations involving molecular self-assembly carried out at the interface between an organic liquid and highly oriented pyrolytic graphite (HOPG). HOPG is a 3D material consisting of stacked graphene layers. Clean and extended atomically flat terraces can be obtained by simply cleaving HOPG using adhesive tape. The structural similarity of graphite surface to graphene makes it an excellent model surface for the self-assembly of molecules on graphene.[9] Moreover, there is a wealth of information available on molecular self-assembly on HOPG,[32,35,36] at the liquid–solid interface as well as under ambient conditions. A typical experiment involves application of a few microliters of a solution containing the molecules of interest on HOPG. The self-assembled networks are formed at the solution–HOPG interface. STM visualization can be carried out at the liquid–solid interface or on dry samples prepared by evaporation of the solvent. Given the epitaxial relationship between alkyl chains and the lattice of graphite, many alkyl-substituted molecules are known to form highly crystalline monolayers on HOPG.[35]

In previous studies carried out in our group, dehydrobenzo[12]annulene (DBA) derivatives have emerged as versatile building blocks for constructing 2D porous networks at the liquid–HOPG interface.[37−46] These molecules consist of a rigid triangular core, the so-called DBA unit, which is typically substituted with six alkyl or alkoxy chains to guide the self-assembly on graphite (Figure 1A). Remarkably, under controlled concentration conditions, these molecules self-assemble into regular nanoporous networks, stabilized by molecule–molecule and molecule–substrate interactions: alkyl chains of adjacent molecules are interdigitated and alkyl chains align along one of the major symmetry axes of graphite. The self-assembled porous networks of DBA are stable and the process of network formation itself is extremely adaptive to synthetic modifications introduced in the peripheral alkyl chains. For example, by altering the length of the alkoxy chains, honeycomb networks of different pore sizes have been realized on HOPG;[38−45] by modifying the alkyl chain terminal groups, tuning of the pore functionality has been demonstrated;[46] by introducing chiral centers in the DBA alkoxy chains, the chirality of the porous networks could be controlled.[45]

In this contribution, we exploit the stable self-assembling properties of DBA derivatives to functionalize graphene supported on various substrates. After confirming the stable and highly ordered network formation of a typical DBA derivative (**DBA-OC12**) on E-G/SiC, we employed a large DBA derivative with diacetylene units in the alkyl chains (**DBA-DA25**) for functionalization
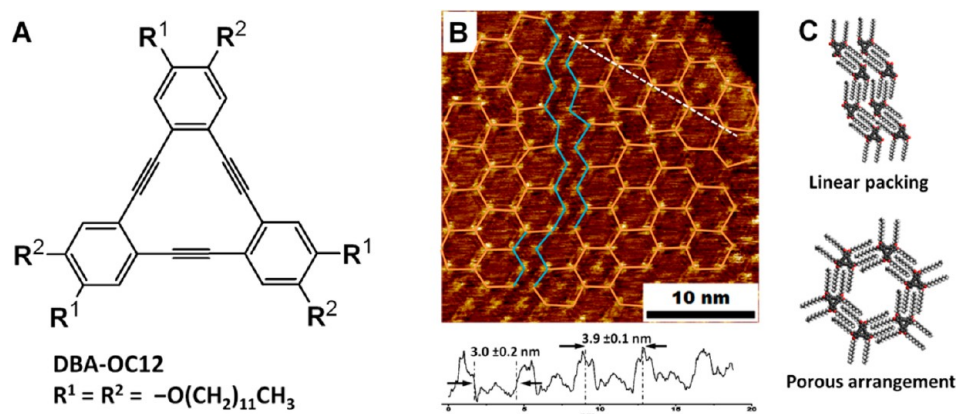
Figure 1. (A) Molecular structure of DBA-OC12. (B) STM image of a monolayer of DBA-OC12 at the interface between TCB and E-G/SiC. Imaging conditions: I_{set} = 100 pA; V_{set} = −950 mV. A line profile along the white dashed line is shown below the STM image. The blue and orange outlines highlight the linear packing and the porous arrangement, respectively. (C) Molecular models for linear packing and porous arrangement of DBA-OC12 observed at the TCB−E-G/SiC interface.

of graphene. The increased stability offered by the diacetylene moieties enables robust network formation under various conditions and on a variety of graphene substrates. A regular nanoporous network with a pore diameter of 5.7 nm was achieved. STM and atomic force microscopy (AFM) investigations reveal that the self-assembled networks formed by **DBA-DA25** are highly flexible and follow the graphene topography without any discontinuity irrespective of the step-edges present in the substrate underneath. Remarkably, such large-pore honeycomb networks are exceptionally stable, both at the liquid−solid interface and under ambient dry conditions.

RESULTS AND DISCUSSION

Graphene samples supported on three different substrates, hence with distinct surface topologies, were investigated. These include epitaxial few-layer graphene grown on SiC,[23,25] CVD-grown single-layer graphene on polycrystalline Cu film on silicon wafer,[33,34] and mechanically exfoliated small single-layer graphene sheets on a mica substrate.[5] AFM and STM measurements were used to evaluate the morphologies of E-G/SiC and CVD-G/Cu surfaces (Figure S1) prior to the deposition of DBAs. The E-G/SiC substrate consists of steps, steep slopes, and flat terraces with areas up to hundreds of square nanometers and provides a suitable surface for the self-assembly of molecules and STM imaging (Figure S1A,B). On the other hand, CVD-G/Cu shows a relatively rough surface and consists of uneven grain-like features reflecting the topography of the underlying polycrystalline Cu film (Figure S1D,E). STM studies of molecular assembly typically require ultraflat surfaces; therefore atomically flat HOPG[32,35,36,42,47] and single-crystalline metal substrates such as Au,[48,49] Ag,[50,51] and Cu[52−55] are the most favorable surfaces used in STM studies. The coarse-grained nature of CVD-G/Cu surfaces (RMS

roughness up to 25.6 nm in a typical AFM image, Figure S1D) may pose challenges for the molecular self-assembly, as well as for the visualization. Therefore, our initial efforts were focused on using E-G/SiC as the substrate, which is relatively less rough (RMS roughness 4.2 nm in a typical AFM image, Figure S1A). **DBA-OC12** (Figure 1A), which is a well-studied building block, was chosen to verify the possibility of DBAs to self-assemble into 2D porous networks on graphene.

In contrast to UHV deposition of organic molecules, which requires an elaborate sample preparation, our approach involves simple drop casting of a 1,2,4-trichlorobenzene (TCB) solution of **DBA-OC12** ($\sim 1 \times 10^{-3}$ M) onto E-G/SiC. STM imaging carried out at the TCB−E-G/SiC interface reveals that the **DBA-OC12** molecules are able to form well-ordered 2D porous networks with a pore size of $\sim$3 nm on the E-G/SiC surface (Figure 1B). A more densely packed linear structure was also visualized. This observation is in agreement with the coexistence of porous and linear packing at high concentration ($>7.4 \times 10^{-4}$ M) observed on HOPG[39] and indicates that the self-assembly process on graphene is not all that different from that on graphite. Although in principle, the diameter of the pores can be increased by altering the length of the alkoxy chains, the DBA derivatives with longer alkoxy chains show stronger concentration dependency. This becomes a serious issue, especially upon solvent evaporation, in which case there is a higher propensity to form densely packed networks.[39]

Aiming at the formation of networks with large pores for which the stability does not depend significantly on the diameter of the pores and the molecular concentration in solution, we moved on to the study of a new type of DBA derivative (**DBA-DA25**; Figure 2A). This DBA derivative not only is substituted with long alkoxy chains but also contains special type of alkoxy chain that possesses diacetylene units. The diacetylene
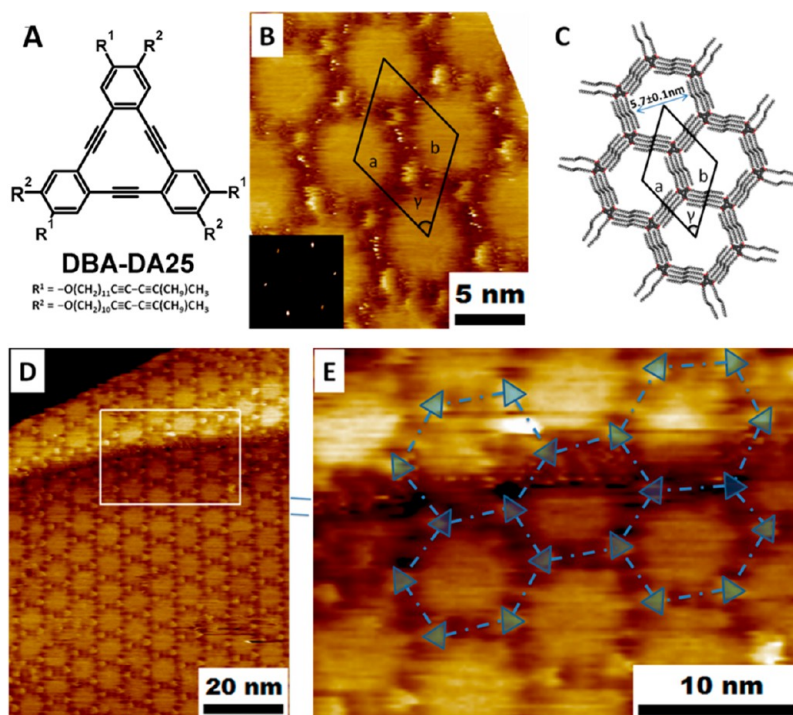
Figure 2. (A) Molecular structure of DBA-DA25. (B) High-resolution STM image of the honeycomb pattern of DBA-DA25 assembled at the interface between epitaxial graphene (E-G/SiC) and TCB. The inset shows the corresponding fast Fourier transform of the E-G/SiC substrate. (C) Molecular model of the honeycomb pattern; unit cell: $a = 7.0 \pm 0.2$ nm, $b = 7.1 \pm 0.2$ nm, and $\gamma = 60 \pm 3°$. The DBA-DA network was found to be rotated by about 23° with respect to the underlying graphene lattice. (D) Large-area STM image of the honeycomb pattern of DBA-DA25 assemblies at the TCB and E-G/SiC interface. (E) Enlarged STM image of the area marked with the white rectangle in D, showing that the 2D porous network seamlessly crosses a step. Blue triangles highlight the DBA cores. Blue dashed lines indicate the alkoxy chains in between the DBA cores. Imaging conditions: $I_{set} = 120$ pA; $V_{set} = -850$ mV.

units are known to provide increased stability to supramolecular networks due to additional interactions based on shape complementarity between kinked alkyl chains.[56,57] A very recent STM study (Figure S2) carried out by us shows that **DBA-DA25** forms well-ordered 2D honeycomb networks at the TCB/HOPG interface. This full report on the design, synthesis, and self-assembly properties including the stability of **DBA-DA25** on HOPG will be presented elsewhere.[58] Here, we focus on the self-assembly properties in relation to the nature of the graphene surface.

To explore the self-assembly on graphene, a solution of **DBA-DA25** (5 μL, ~2 × 10^{-6} M in TCB) was applied to E-G/SiC or CVD-G/Cu substrate predited into dimensions of ~0.5 × 1.0 cm^2. **DBA-DA25** molecules were observed to self-assemble into a porous honeycomb structure at the TCB−E-G/SiC interface (Figure 2). The bright triangular features correspond to the annulene cores of **DBA-DA25**, while the dark features bridging the cores are the regions where the alkoxy chains are adsorbed. The less bright features in the middle of the alkoxy chains correspond to the diacetylene units. A high-resolution STM image of the honeycomb network is shown in Figure 2B. The orientation of the diacetylene-containing chains coincides with the symmetry axes of the underlying graphene lattice, indicating

good epitaxial registry. Simple as well as substituted alkanes and alkyl chain containing molecules are known to exhibit such registry on HOPG substrate. The periodicity of the pores (7.0 ± 0.1 nm) as well as the orientation of the **DBA-DA25** unit cell with respect to the graphene lattice is consistent with the results obtained on HOPG (Figure S2). These observations are again indicative of the similarities in the supramolecular network formation on HOPG and graphene. Thus, similar to HOPG, the supramolecular networks of **DBA-DA25** on graphene are also stabilized by interdigitation between pairs of alkoxy chains involving adjacent molecules. The pore size reaches up to 5.7 ± 0.1 nm (the edge-to-edge distance as indicated in Figure 2C).

Despite the obvious similarities, there are some peculiar differences in the self-assembly behavior on graphene and graphite. The most important difference is the behavior of the supramolecular networks at the step-edges. In the case of HOPG, the **DBA-DA25** networks are typically discontinuous across step-edges. In other words, a step-edge on HOPG interrupts the domain, and each terrace consists of a separate domain (Figure S3 in the Supporting Information). On the contrary, **DBA-DA25** networks were found to be in full compliance with the underlying graphene topography and seamlessly crossed surface steps (Figure 2D and E).

Figure 2E shows the enlarged STM image of the area indicated in Figure 2D, demonstrating that the DBA nanomesh grows over a step-edge inherited from the underlying SiC substrate. These observations clearly demonstrate that the graphene layer continuously covers the step-edge present in the SiC substrate underneath. A similar phenomenon was reported earlier for monolayers of rigid polyaromatic molecules such as PTCDA,[23−27] PTCDI,[25,28] and phthalocyanines[29−31] as well as for those formed by relatively flexible aliphatic molecules such as pentacosadiynoic acid[22] on graphene surface observed under UHV conditions. The present case stands out from those reported in the literature due to much lower surface density of the building blocks involved. These results when considered in the context of those obtained in the past reveal that the formation of continuous domains over step-edges is not a property of a given molecular system but is rather inherent to the graphene−substrate combination.

These encouraging observations prompted us to explore the self-assembly behavior of **DBA-DA25** on rougher graphene surfaces such as CVD-G/Cu. Remarkably, well-organized 2D porous networks were also observed (Figure 3A) on CVD-G/Cu despite its higher surface roughness. The STM image provided in Figure 3B reveals that the porous network consists of **DBA-DA25** exhibiting a similar arrangement as that observed on E-G/SiC. To the best of our knowledge, this is the first observation of an ordered 2D porous network on such a highly rough graphene surface under ambient conditions. Similar to the observations made for E-G/SiC, the **DBA-DA25** molecules assemble into an extended nanomesh on the CVD-G/Cu surface, which follows the topography of the CVD-G/Cu surface without any obvious disruption by the roughness of the underlying graphene. The robustness of the monolayer films is attributed to strong self-assembling properties of **DBA-DA25**. The long alkoxy chains offer the flexibility to adapt to the graphene topography and provide sufficient interaction with graphene *via* vdW interactions. Meanwhile, the interdigitation between the long alkoxy chains of neighboring **DBA-DA25** molecules provides intermolecular stabilization *via* vdW interactions to form an extended stable network. The presence of diacetylene units further enhances the stability of the 2D networks.

While the DBA assemblies are readily observed at the interface between TCB and CVD-G/Cu, the substrate roughness adversely affects the imaging. High-resolution STM images of **DBA-DA25** at the TCB/CVD-G interface are far more difficult to obtain compared to those at TCB/E-G interface. Although the structural aspects of the **DBA-DA25** networks formed on CVD-G are similar to those on HOPG, we noted that the self-assembly proceeds at relatively slower rate on CVD-G than that on HOPG. For a given solution concentration,
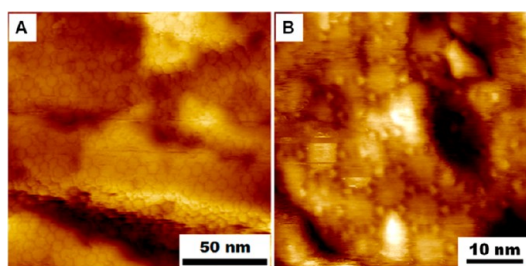

Figure 3. STM images of DBA-DA25 self-assembled at the TCB−CVD-G/Cu interface. (A) Large-area STM image and (B) small-scale image of the DBA-DA25 honeycombs clearly illustrating the compliance of the nanomesh to the graphene substrate, regardless of the surface roughness. Imaging conditions: I_{set} = 100 pA; V_{set} = −950 mV.

porous **DBA-DA25** networks were instantaneously formed on HOPG, whereas on CVD-G, an equilibration period of *ca.* 15 min was typically necessary before the stable self-assembled networks could be obtained. This decrease in the rate of the assembly process could be related to the roughness of graphene compared to HOPG. Linear packing was occasionally seen to coexist with the honeycomb networks formed on CVD-G/Cu, which is not the case for the networks obtained on HOPG from solutions with the same concentration. At this point, it is not clear if this is due to the differences in surface roughness or that other aspects are at play.

To evaluate the stability of these unique porous molecular assemblies under ambient dry conditions, the solvent was removed by gentle rinsing with water followed by drying under a flow of N_2. Since water could dissolve neither TCB nor DBA molecules, TCB and excess DBA molecules dissolved in TCB are expected to be removed from the substrate *via* solvent repulsion. According to this logic, the self-assembled **DBA-DA25** networks should remain on the surface thanks to their interaction with the substrate and hydrophobic nature. Due to the higher roughness of the graphene samples, the drying protocol was first verified on HOPG. STM investigations confirmed that the DBA honeycomb network survived on HOPG after the solvent removal steps (Figure S4A). However, some DBA molecules were found missing from the network. Additional STM imaging revealed that the scanning STM tip could perturb the self-assembled DBA network under ambient conditions and induce molecular desorption. Figure S4B provided in the Supporting Information reveals that the reimaged area marked with dotted lines at the upper-left corner of the image shows that the DBA molecules were completely removed by the STM tip. In contrast, AFM imaging performed on the same sample showed a well-preserved DBA honeycomb network after the solvent removal steps. No obvious defects were observed in the entire network (Figure S4C and D). These observations clearly indicate that the defects in the DBA honeycomb monolayer result from the STM imaging rather than the solvent removal steps.
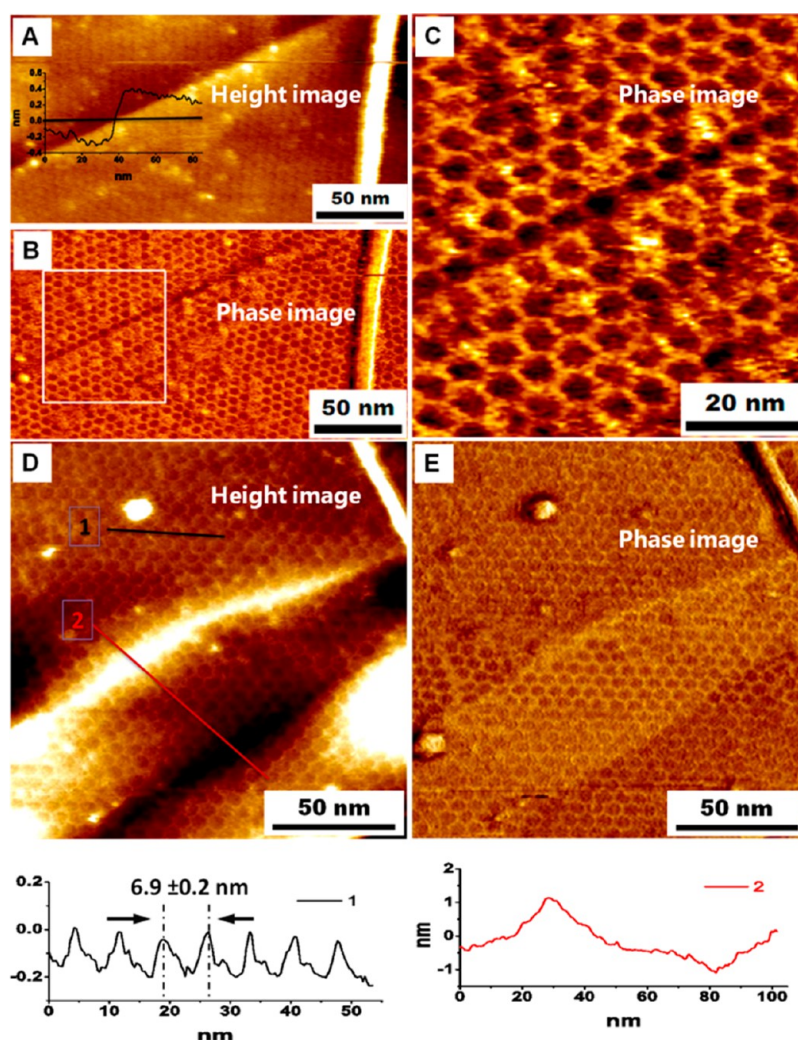
Figure 4. AFM images of DBA-DA25 self-assembled monolayer on E-G/SiC under ambient conditions. (A) Height image and (B) corresponding phase image, showing a continuous honeycomb structure crossing over a ~0.7 nm high step-edge on E-G/SiC. (C) Enlarged AFM phase image of the same area marked with the white square box in B clearly showing the DBA honeycomb network without any discontinuity at the step-edge. (D and E) DBA-DA25 porous networks demonstrating compliance with a steep slope of the graphene substrate. Line profiles along the black line (1) and the red line (2) in D are shown below the STM images, in which profile 1 indicates that the periodicity of the pores is about 6.9 ± 0.2 nm and profile 2 shows the significant topographical changes of the steep slope, respectively.

To avoid such desorption effects induced by STM imaging, tapping mode AFM becomes the natural choice for the investigation of the stability and uniformity of the dry DBA porous networks on graphene due to reduced lateral forces exerted by the AFM tip. Similar to the results obtained on HOPG, the DBA porous networks were found to survive on E-G/SiC under ambient conditions after the aforementioned solvent removal step. The AFM images in Figure 4 demonstrate that the dry network remained intact even at graphene step-edges (Figure 4A, B, and C) and steep slope regions (Figure 4D and E), showing no discontinuity. No obvious difference was found between the AFM images for dry DBA networks and the earlier STM images obtained at the TCB−E-G/SiC interface. The periodicity of the pores as obtained from AFM measurements is about 6.9 ± 0.2 nm (Figure 4D), consistent with the molecular model and previous STM measurements.

Multipoint measurements at different locations across the sample confirmed the complete coverage of graphene by the molecular nanomesh. The absence of obvious defects and aggregates (see large-area AFM images, Figure S5) confirms the uniformity and continuity of the DBA porous network on E-G/SiC. It is worth noting that no obvious changes in the morphology were detected after standing in ambient air for 2 weeks, illustrating the stability and robustness of the DBA honeycomb networks in air.

Finally, the self-assembled network formation of **DBA-DA25** was also investigated on M-G/Mica. AFM images provided in Figure 5 indicate that **DBA-DA25** forms a highly ordered porous phase on exfoliated graphene, whereas on bare mica it exhibits a distinctively disordered morphology. These observations imply that the formation of the DBA nanomesh is templated by graphene.
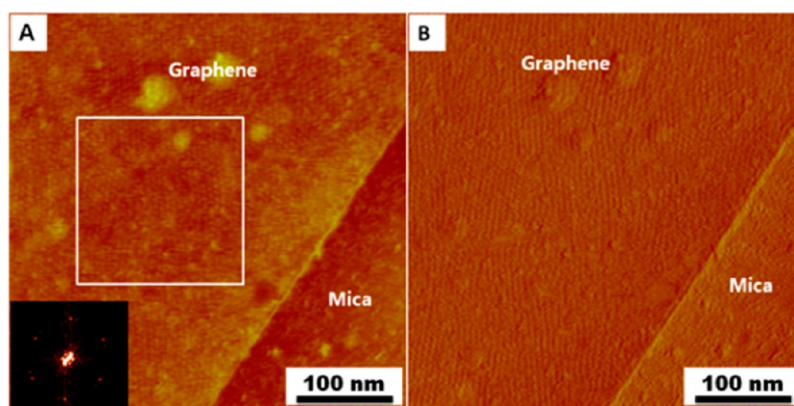
Figure 5. AFM images of a monolayer of DBA-DA25 on M-G/Mica. (A) Height image and (B) corresponding phase image, respectively. The inset in A is the fast Fourier transform of the white square area in A showing the well-defined periodicity of the DBA assemblies.

CONCLUSIONS AND OUTLOOK

We have identified a novel building block in the form of **DBA**, which upon physisorption, leads to formation of stable nanoporous self-assembled networks on different graphene substrates. Identification of such building blocks that can form stable supramolecular networks across diverse graphene substrates is essential, as every application needs a given type of graphene substrate. The two DBA derivatives discussed in this study furnished supramolecular networks with periodicities of 3.9 nm (**DBA-OC12**) and 7.0 nm (**DBA-DA25**). However, as demonstrated by us earlier, these two numbers do not represent the limit by any means, and well-ordered networks with varying periodicities have been fabricated on HOPG using these building blocks. This knowledge is easily transferrable to graphene, as demonstrated in the case of **DBA-OC12** and **DBA-DA25**. Given the fact that the periodicity, the pore diameter, and the functionality of the DBA pore can be easily controlled by synthetic modification of the peripheral chains, these building blocks hold promise in the tunable functionalization of various graphene substrates. Furthermore, the cavities of these networks could be readily occupied by a variety of guest molecules. This aspect could be exploited for controlled and periodic functionalization of graphene using multicomponent host–guest type networks or for graphene-based sensing devices. The robust air-stable networks of **DBA-DA25** are particularly interesting since they possess polymerizable diacetylene units. Attempts are in progress to polymerize these supramolecularly assembled networks to realize a one molecule thick nanoporous covalent organic network (COF) on graphene surface. Such well-ordered nanoporous COFs confined against the graphene surface are expected to open further possibilities of such graphene composites in various applications.

EXPERIMENTAL SECTION

The synthesis of **DBA-OC12** was described previously.[39] The synthesis of **DBA-DA25** will be reported elsewhere.[58] To form self-assembled monolayers of the DBA derivatives at the liquid–solid interface, a drop (5 μL) of a diluted TCB solution containing the DBA derivative of interest was applied on the substrate of a freshly cleaved HOPG or prediced E-G/SiC, CVD-G/Cu, or M-G/Mica. After drop casting the solution, the STM imaging was carried out immediately by using mechanically cut Pt/Ir (80%/20%) tips either on a PicoSPM (Agilent) or on a Nanoscope IIID (Veeco Instruments) at room temperature (20–25 °C). To ensure electrical contact with graphene, metal wires were used to connect the E-G/SiC and CVD-G/Cu substrates from the top. Dry monolayer assemblies on E-G/SiC and on M-G/Mica were prepared by removal of TCB solvent from the substrates by gentle rinsing with water followed by drying under a stream of N_2. AFM imaging was performed using a Multimode SPM (DI) with a Nanoscope IV controller. The AFM images were acquired in tapping mode under ambient air conditions with silicon cantilevers (spring constant of 21–60 N/m, resonance frequency of ca. 300 kHz, Olympus, Japan). Scanning Probe Image Processor (SPIP) software (Image Metrology ApS) was used for image analysis and drift correction of the high-resolution STM images.

REFERENCES AND NOTES

1. Novoselov, K. S.; Geim, A. K.; Morozov, S. V.; Jiang, D.; Zhang, Y.; Dubonos, S. V.; Grigorieva, I. V.; Firsov, A. A. Electric Field Effect in Atomically Thin Carbon Films. *Science* **2004**, *306*, 666–669.

2. Geim, A. K. Graphene: Status and Prospects. *Science* **2009**, *324*, 1530–1534.

3. Lin, Y. M.; Dimitrakopoulos, C.; Jenkins, K. A.; Farmer, D. B.; Chiu, H. Y.; Grill, A.; Avouris, P. 100-GHz Transistors from Wafer-Scale Epitaxial Graphene. *Science* **2010**, *327*, 662–662.

4. Huang, X.; Qi, X. Y.; Boey, F.; Zhang, H. Graphene-Based Composites. *Chem. Soc. Rev.* **2012**, *41*, 666–686.

5. Xu, K.; Cao, P. G.; Heath, J. R. Graphene Visualizes the First Water Adlayers on Mica at Ambient Conditions. *Science* **2010**, *329*, 1188–1191.

6. Colson, J. W.; Woll, A. R.; Mukherjee, A.; Levendorf, M. P.; Spitler, E. L.; Shields, V. B.; Spencer, M. G.; Park, J.; Dichtel, W. R. Oriented 2D Covalent Organic Framework Thin Films on Single-Layer Graphene. *Science* **2011**, *332*, 228–231.

7. Li, B.; Cao, X.; Ong, H. G.; Cheah, J. W.; Zhou, X.; Yin, Z.; Li, H.; Wang, J.; Boey, F.; Huang, W.; *et al*. All-Carbon Electronic Devices Fabricated by Directly Grown Single-Walled Carbon Nanotubes on Reduced Graphene Oxide Electrodes. *Adv. Mater.* **2010**, *22*, 3058–3061.

8. Dai, L. Functionalization of Graphene for Efficient Energy Conversion and Storage. *Acc. Chem. Res.* **2013**, *46*, 31–42. Several other review papers on graphene synthesis, properties, and applications can be found in the same issue.

9. Zhang, T.; Cheng, Z. G.; Wang, Y. B.; Li, Z. J.; Wang, C. X.; Li, Y. B.; Fang, Y. Self-Assembled 1-Octadecanethiol Monolayers on Graphene for Mercury Detection. *Nano Lett.* **2010**, *10*, 4738–4741.

10. Li, B.; Klekachev, A. V.; Cantoro, M.; Huyghebaert, C.; Stesmans, A.; Asselberghs, I.; De Gendt, S.; De Feyter, S. Toward Tunable Doping in Graphene FETs by Molecular Self-Assembled Monolayers. *Nanoscale* **2013**, *5*, 9640–9644.

11. Bai, J. W.; Zhong, X.; Jiang, S.; Huang, Y.; Duan, X. F. Graphene Nanomesh. *Nat. Nanotechnol.* **2010**, *5*, 190–194.

12. Liang, Y. T.; Hersam, M. C. Towards Rationally Designed Graphene-Based Materials and Devices. *Macromol. Chem. Phys.* **2012**, *213*, 1091–1100.

13. Yu, W. J.; Liao, L.; Chae, S. H.; Lee, Y. H.; Duan, X. Toward Tunable Band Gap and Tunable Dirac Point in Bilayer Graphene with Molecular Doping. *Nano Lett.* **2011**, *11*, 4759–4763.

14. Szafranek, B. N.; Schall, D.; Otto, M.; Neumaier, D.; Kurz, H. High On/Off Ratios in Bilayer Graphene Field Effect Transistors Realized by Surface Dopants. *Nano Lett.* **2011**, *11*, 2640–2643.

15. Prado, M. C.; Nascimento, R.; Moura, L. G.; Matos, M. J. S.; Mazzoni, M. S. C.; Cancado, L. G.; Chacham, H.; Neves, B. R. A. Two-Dimensional Molecular Crystals of Phosphonic Acids on Graphene. *ACS Nano* **2011**, *5*, 394–398.

16. Dong, X.; Shi, Y.; Zhao, Y.; Chen, D.; Ye, J.; Yao, Y.; Gao, F.; Ni, Z.; Yu, T.; Shen, Z.; *et al*. Symmetry Breaking of Graphene Monolayers by Molecular Decoration. *Phys. Rev. Lett.* **2009**, *102*, 135501–135504.

17. Georgakilas, V.; Otyepka, M.; Bourlinos, A. B.; Chandra, V.; Kim, N.; Kemp, K. C.; Hobza, P.; Zboril, R.; Kim, K. S. Functionalization of Graphene: Covalent and Non-Covalent Approaches, Derivatives and Applications. *Chem. Rev.* **2012**, *112*, 6156–6214.

18. Bekyarova, E.; Sarkar, S.; Wang, F. H.; Itkis, M. E.; Kalinina, I.; Tian, X. J.; Haddon, R. C. Effect of Covalent Chemistry on the Electronic Structure and Properties of Carbon Nanotubes and Graphene. *Acc. Chem. Res.* **2013**, *46*, 65–76.

19. Sarkar, S.; Bekyarova, E.; Haddon, R. C. Chemistry at the Dirac Point: Diels Alder Reactivity of Graphene. *Acc. Chem. Res.* **2012**, *45*, 673–682.

20. Wu, J.; Xie, L.; Li, Y.; Wang, H.; Ouyang, Y.; Guo, J.; Dai, H. Controlled Chlorine Plasma Reaction for Noninvasive Graphene Doping. *J. Am. Chem. Soc.* **2011**, *133*, 19668–19671.

21. Withers, F.; Bointon, T. H.; Dubois, M.; Russo, S.; Craciun, M. F. Nanopatterning of Fluorinated Graphene by Electron Beam Irradiation. *Nano Lett.* **2011**, *11*, 3912–3916.

22. Deshpande, A.; Sham, C.-H.; Alaboson, J. M. P.; Mullin, J. M.; Schatz, G. C.; Hersam, M. C. Self-Assembly and Photopolymerization of Sub-2 nm One-Dimensional Organic Nanostructures on Graphene. *J. Am. Chem. Soc.* **2012**, *134*, 16759–16764.

23. Wang, Q. H.; Hersam, M. C. Room-Temperature Molecular-Resolution Characterization of Self-Assembled Organic Monolayers on Epitaxial Graphene. *Nat. Chem.* **2009**, *1*, 206–211.

24. Emery, J. D.; Wang, Q. H.; Zarrouati, M.; Fenter, P.; Hersam, M. C.; Bedzyk, M. J. Structural Analysis of PTCDA Monolayers on Epitaxial Graphene with Ultra-High Vacuum Scanning Tunneling Microscopy and High-Resolution X-Ray Reflectivity. *Surf. Sci.* **2011**, *605*, 1685–1693.

25. Wang, Q. H.; Hersam, M. C. Nanofabrication of Heteromolecular Organic Nanostructures on Epitaxial Graphene *via* Room Temperature Feedback-Controlled Lithography. *tNano Lett.* **2011**, *11*, 589–593.

26. Huang, H.; Chen, S.; Gao, X.; Chen, W.; Wee, A. T. S. Structural and Electronic Properties of PTCDA Thin Films on Epitaxial Graphene. *ACS Nano* **2009**, *3*, 3431–3436.

27. Lauffer, P.; Emtsev, K. V.; Graupner, R.; Seyller, T.; Ley, L. Molecular and Electronic Structure of PTCDA on Bilayer Graphene on SiC(0001) Studied with Scanning Tunneling Microscopy. *Phys. Status Solidi B* **2008**, *245*, 2064–2067.

28. Pollard, A. J.; Perkins, E. W.; Smith, N. A.; Saywell, A.; Goretzki, G.; Phillips, A. G.; Argent, S. P.; Sachdev, H.; Muller, F.; Hufner, S.; *et al*. Supramolecular Assemblies Formed on an Epitaxial Graphene Superstructure. *Angew. Chem., Int. Ed.* **2010**, *49*, 1794–1799.

29. Xiao, K.; Deng, W.; Keum, J. K.; Yoon, M.; Vlassiouk, I. V.; Clark, K. W.; Li, A. P.; Kravchenko, I. I.; Gu, G.; Payzant, E. A.; *et al*. Surface-Induced Orientation Control of CuPc Molecules for the Epitaxial Growth of Highly Ordered Organic Crystals on Graphene. *J. Am. Chem. Soc.* **2013**, *135*, 3680–3687.

30. Ogawa, Y.; Niu, T. C.; Wong, S. L.; Tsuji, M.; Wee, A. T. S.; Chen, W.; Ago, H. Self-Assembly of Polar Phthalocyanine Molecules on Graphene Grown by Chemical Vapor Deposition. *J. Phys. Chem. C* **2013**, 10.1021/jp406681j.

31. Jarvinen, P.; Hamalainen, S. K.; Banerjee, K.; Hakkinen, P.; Ijas, M.; Harju, A.; Liljeroth, P. Molecular Self-Assembly on Graphene on SiO_2 and h-BN Substrates. *Nano Lett.* **2013**, *13*, 3199–3204.

32. Lei, S. B.; Tahara, K.; Adisoejoso, J.; Balandina, T.; Tobe, Y.; De Feyter, S. Towards Two-Dimensional Nanoporous Networks: Crystal Engineering at the Solid-Liquid Interface. *CrystEngComm* **2010**, *12*, 3369–3381.

33. Wang, Y.; Zheng, Y.; Xu, X.; Dubuisson, E.; Bao, Q.; Lu, J.; Loh, K. P. Electrochemical Delamination of CVD-Grown Graphene Film: Toward the Recyclable Use of Copper Catalyst. *ACS Nano* **2011**, *5*, 9927–9933.

34. Li, X.; Cai, W.; An, J.; Kim, S.; Nah, J.; Yang, D.; Piner, R.; Velamakanni, A.; Jung, I.; Tutuc, E. Large-Area Synthesis of High-Quality and Uniform Graphene Films on Copper Foils. *Science* **2009**, *324*, 1312–1314.

35. De Feyter, S.; De Schryver, F. C. Two-Dimensional Supramolecular Self-Assembly Probed by Scanning Tunneling Microscopy. *Chem. Soc. Rev.* **2003**, *32*, 139–150.

36. Elemans, J. A. A. W.; Lei, S.; De Feyter, S. Molecular and Supramolecular Networks on Surfaces: From Two-Dimensional Crystal Engineering to Reactivity. *Angew. Chem., Int. Ed.* **2009**, *48*, 7298–7332.

37. Lei, S. B.; Tahara, K.; Mullen, K.; Szabelski, P.; Tobe, Y.; De Feyter, S. Mixing Behavior of Alkoxylated Dehydrobenzo[12]annulenes at the Solid-Liquid Interface: Scanning Tunneling Microscopy and Monte Carlo Simulations. *ACS Nano* **2011**, *5*, 4145–4157.

38. Adisoejoso, J.; Tahara, K.; Lei, S. B.; Szabelski, P.; Rzysko, W.; Inukai, K.; Blunt, M. O.; Tobe, Y.; De Feyter, S. One Building Block, Two Different Nanoporous Self-Assembled Monolayers: A Combined STM and Monte Carlo Study. *ACS Nano* **2012**, *6*, 897–903.

39. Lei, S. B.; Tahara, K.; De Schryver, F. C.; Van der Auweraer, M.; Tobe, Y.; De Feyter, S. One Building Block, Two Different Supramolecular Surface-Confined Patterns: Concentration in Control at the Solid-Liquid Interface. *Angew. Chem., Int. Ed.* **2008**, *47*, 2964–2968.

40. Adisoejoso, J.; Tahara, K.; Okuhata, S.; Lei, S.; Tobe, Y.; De Feyter, S. Two-Dimensional Crystal Engineering: A Four-Component Architecture at a Liquid-Solid Interface. *Angew. Chem., Int. Ed.* **2009**, *48*, 7353–7357.

41. Lei, S. B.; Tahara, K.; Feng, X. L.; Furukawa, S. H.; De Schryver, F. C.; Mullen, K.; Tobe, Y.; De Feyter, S. Molecular Clusters in Two-Dimensional Surface-Confined Nanoporous Molecular Networks: Structure, Rigidity, and Dynamics. *J. Am. Chem. Soc.* **2008**, *130*, 7119–7129.

42. Tahara, K.; Furukawa, S.; Uji-I, H.; Uchino, T.; Ichikawa, T.; Zhang, J.; Mamdouh, W.; Sonoda, M.; De Schryver, F. C.; De Feyter, S.; *et al.* Two-Dimensional Porous Molecular Networks of Dehydrobenzo[12]annulene Derivatives *via* Alkyl Chain Interdigitation. *J. Am. Chem. Soc.* **2006**, *128*, 16613–16625.

43. Blunt, M. O.; Adisoejoso, J.; Tahara, K.; Katayama, K.; Van der Auweraer, M.; Tobe, Y.; De Feyter, S. Temperature-Induced Structural Phase Transitions in a Two-Dimensional Self-Assembled Network. *J. Am. Chem. Soc.* **2013**, *135*, 12068–12075.

44. Lei, S.; Surin, M.; Tahara, K.; Adisoejoso, J.; Lazzaroni, R.; Tobe, Y.; De Feyter, S. Programmable Hierarchical Three-Component 2D Assembly at a Liquid-Solid Interface: Recognition, Selection, and Transformation. *Nano Lett.* **2008**, *8*, 2541–2546.

45. Tahara, K.; Yamaga, H.; Ghijsens, E.; Inukai, K.; Adisoejoso, J.; Blunt, M. O.; De Feyter, S.; Tobe, Y. Control and Induction of Surface-Confined Homochiral Porous Molecular Networks. *Nat. Chem.* **2011**, *3*, 714–719.

46. Tahara, K.; Inukai, K.; Adisoejoso, J.; Yamaga, H.; Balandina, T.; Blunt, M. O.; De Feyter, S.; Tobe, Y. Tailoring Surface-Confined Nanopores with Photoresponsive Groups. *Angew. Chem., Int. Ed.* **2013**, *52*, 8373–8376.

47. Kudernac, T.; Lei, S. B.; Elemans, J.; De Feyter, S. Two-Dimensional Supramolecular Self-Assembly: Nanoporous Networks on Surfaces. *Chem. Soc. Rev.* **2009**, *38*, 402–421.

48. Madueno, R.; Raisanen, M. T.; Silien, C.; Buck, M. Functionalizing Hydrogen-Bonded Surface Networks with Self-Assembled Monolayers. *Nature* **2008**, *454*, 618–621.

49. Zhong, D. Y.; Franke, J. H.; Podiyanachari, S. K.; Blomker, T.; Zhang, H. M.; Kehr, G.; Erker, G.; Fuchs, H.; Chi, L. F. Linear Alkane Polymerization on a Gold Surface. *Science* **2011**, *334*, 213–216.

50. Glockler, K.; Seidel, C.; Soukopp, A.; Sokolowski, M.; Umbach, E.; Bohringer, M.; Berndt, R.; Schneider, W. D. Highly Ordered Structures and Submolecular Scanning Tunnelling Microscopy Contrast of PTCDA and DM-PBDCI Monolayers on Ag(111) and Ag(110). *Surf. Sci.* **1998**, *405*, 1–20.

51. Kuhne, D.; Klappenberger, F.; Decker, R.; Schlickum, U.; Brune, H.; Klyatskaya, S.; Ruben, M.; Barth, J. V. Self-Assembly of Nanoporous Chiral Networks with Varying Symmetry from Sexiphenyl-Dicarbonitrile on Ag(111). *J. Phys. Chem. C* **2009**, *113*, 17851–17859.

52. Schunack, M.; Petersen, L.; Kuhnle, A.; Laegsgaard, E.; Stensgaard, I.; Johannsen, I.; Besenbacher, F. Anchoring of Organic Molecules to a Metal Surface: HtBDC on Cu(110). *Phys. Rev. Lett.* **2001**, *86*, 456–459.

53. Payer, D.; Comisso, A.; Dmitriev, A.; Strunskus, T.; Lin, N.; Woll, C.; DeVita, A.; Barth, J. V.; Kern, K. Ionic Hydrogen Bonds Controlling Two-Dimensional Supramolecular Systems at a Metal Surface. *Chem.—Eur. J.* **2007**, *13*, 3900–3906.

54. Chen, Q.; Frankel, D. J.; Richardson, N. V. Organic Adsorbate Induced Surface Reconstruction: p-Aminobenzoic Acid on Cu(110). *Langmuir* **2001**, *17*, 8276–8280.

55. Wan, L. J.; Itaya, K. *In Situ* Scanning Tunnelling Microscopy of Benzene, Naphthalene, and Anthracene Adsorbed on Cu(111) in Solution. *Langmuir* **1997**, *13*, 7173–7179.

56. Xue, Y.; Zimmt, M. B. Tetris in Monolayers: Patterned Self-Assembly using Side Chain Shape. *Chem. Commun.* **2011**, *47*, 8832–8834.

57. Xue, Y.; Zimmt, M. B. Patterned Monolayer Self-Assembly Programmed by Side Chain Shape: Four-Component Gratings. *J. Am. Chem. Soc.* **2012**, *134*, 4513–4516.

58. Tahara, K.; Adisoejoso, J.; Inukai, K.; Lei, S. Noguchi, A.; Li, B. Vanderlinden, W. De Feyter, S. Tobe, Y. *Harnessing a Diacetylene Unit: A Molecular Design for Porous Two-Dimensional Network Formation by Self-Assembly of Alkoxy Dehydrobenzo[12]annulene Derivatives at the Liquid/Solid Interface*, submitted.